© 2017. Published by The Company of Biologists Ltd | Journal of Experimental Biology (2017) 220, 1423-1434 doi:10.1242/jeb.147108

RESEARCH ARTICLE

Does the membrane pacemaker theory of metabolism explain the size dependence of metabolic rate in marine mussels?

Alexey Sukhotin[1,2,*], Natalia Fokina[3], Tatiana Ruokolainen[3], Christian Bock[4], Hans-Otto Pörtner[4,5] and Gisela Lannig[4]

ABSTRACT

According to the membrane pacemaker theory of metabolism (MPT), allometric scaling of metabolic rate in animals is determined by the composition of cellular and mitochondrial membranes, which changes with body size in a predictable manner. MPT has been elaborated from interspecific comparisons in mammals. It projects that the degree of unsaturation of membrane phospholipids decreases in larger organisms, thereby lowering ion permeability of the membranes and making cellular, and thus whole-animal metabolism more efficient. Here, we tested the applicability of the MPT to a marine ectotherm, the mussel *Mytilus edulis* at the intraspecific level. We determined effects of body mass on whole-organism, tissue and cellular oxygen consumption rates, on heart rate, metabolic enzyme activities and on the lipid composition of membranes. In line with allometric patterns, the organismal functions and processes such as heart rate, whole-animal respiration rate and phospholipid contents showed a mass-dependent decline. However, the allometry of tissue and cellular respiration and activity of metabolic enzymes was poor; fatty acid unsaturation of membrane phospholipids of gill tissue was independent of animal size. It is thus conceivable that most of the metabolic allometry observed at the organismal level is determined by systemic functions. These whole-organism patterns may be supported by energy savings associated with growing cell size but not by structural changes in membranes. Overall, the set of processes contributing to metabolic allometry in ectotherms may differ from that operative in mammals and birds, with a reduced involvement of the mechanisms proposed by the MPT.

KEY WORDS: Allometric scaling, Cells, Fatty acids, Heart rate, Enzyme activity, Cardiac magnetic resonance imaging

INTRODUCTION

The fact that the metabolic rate of living organisms is functionally linked to their body size is known since the 19th century. The pioneering work of Rubner (1883), Kleiber (1932), Brody (1945), Zeuthen (1947), Winberg (1956), Hemmingsen (1960) and others showed a decline of mass-specific metabolic rate (R) with increasing body size (M) according to a power function with a power coefficient varying within relatively narrow limits (−0.35 to −0.25). During the second half of the 20th century, a tremendous body of data was generated to address this relationship in most animal taxa. Virtually all publications show a decline in mass-specific metabolic rate with increasing body size, not only across different taxa, but also across individuals within a species (for a recent review, see Konarzewski and Książek, 2013) and even within individual specimens during their ontogenesis (e.g. Moses et al., 2008; Maino and Kearney, 2014). The observed pattern supports a universal empirical rule, the so-called 'metabolic scaling law' in biology, which postulates that mass-specific metabolic rate is proportional to the body mass of an organism with a power coefficient of −0.25 (Kleiber, 1932; Schmidt-Nielsen, 1984; West et al., 2002). In support of this law, it has been shown that the specific metabolic rates of isolated mammalian cells (cardiac muscle) as well as of mitochondrial isolates (in the presence of substrate and ADP, state 3) declined with increasing animal body size (West et al., 2002; West and Brown, 2005).

These patterns indicate fundamental allometric changes in the rate of cellular metabolism and mitochondrial functioning; however, the mechanistic causes of these differences remain under debate. The phenomenon of 'universal' allometric changes in metabolic rates suggests a unifying principle, and numerous explanations have been proposed. However, no commonly accepted theory exists that satisfactorily explains either the phenomenon of declining mass-specific metabolic rate with body size, or the universal exponent describing this decline. Interest in this problem rose steeply in the 1990 to 2000s and several excellent theories have been proposed (for a few examples see West et al., 1997; Hulbert and Else, 1999; Hochachka et al., 2003; Glazier, 2010; Kooijman, 2010). However, none of these theories has gained wide acceptance (recent reviews: White and Kearney, 2013; Glazier, 2014).

The membrane pacemaker theory of metabolism (MPT, Hulbert and Else, 1999) is one of the most consistent hypotheses to mechanistically explain the size-dependent decline in metabolic rates of homeothermic animals (birds and mammals). This theory links size-dependent changes in the structure and function of cellular and mitochondrial membranes to the efficiency of energy-dependent transport processes that then shape the rate of cellular and organismal energy metabolism. Variations in the structure of cellular and mitochondrial membranes cause various levels of membrane leakiness for ions (cell membrane) or protons (mitochondrial membrane) and associated adjustments in the capacities of ion transport mechanisms (for mitochondrial findings, see Hulbert and Else, 1999, 2000, 2005).

In the late 1970s, Gudbjarnason et al. (1978) found that the levels of polyunsaturated docosahexaenoic acid [22:6 (n-3)] in the membranes of mammalian myocytes decreased with increasing body size. These and similar observations in mammals (Couture and Hulbert, 1995a) led to the formulation of the MPT: the levels of

[1]White Sea Biological Station, Zoological Institute of Russian Academy of Sciences, Saint-Petersburg 199034, Russia. [2]Department of Invertebrate Biology, Saint-Petersburg State University, Saint-Petersburg 199034, Russia. [3]Laboratory for Environmental Biochemistry, Institute of Biology, Karelian Research Centre of Russian Academy of Sciences, Petrozavodsk 185910, Russia. [4]Integrative Ecophysiology, Alfred Wegener Institute Helmholtz Centre for Polar and Marine Research, Bremerhaven D-27570, Germany. [5]University of Bremen, Bremen 28359, Germany.

*Author for correspondence (Alexey.Sukhotin@zin.ru)

A.S., 0000-0003-2626-5317

Received 1 August 2016; Accepted 28 January 2017

Journal of Experimental Biology (2017) 220, 1423-1434 doi:10.1242/jeb.147108

polyunsaturated fatty acids in biomembranes cause body-size-dependent variations in the fluidity and permeability of membranes, thereby setting the rates of membrane-dependent cellular processes and hence whole-animal metabolic rate.

An increase in mammalian body size thus shifts the composition of fatty acids in the phospholipids of cellular and mitochondrial membranes towards increased fatty acid saturation levels. This leads to a decrease in membrane fluidity and permeability, which in turn results in reduced energy expenditure of the processes maintaining transmembrane ion gradients (e.g. Na^+/K^+-ATPase activity, Jimenez et al., 2011) and counteracts the futile cycling of protons through the inner mitochondrial membrane (Porter et al., 1996). Thus, changes in the fatty acid composition, and consequently in the fluidity of membranes, enhance metabolic efficiency at larger body sizes.

Data on the allometry of cellular metabolism in ectothermic vertebrates (lampreys, fish and reptiles) are few. Across-species comparisons result in a classical allometric decline of cellular respiration with increasing body mass (Savina et al., 1997), while such allometry has not been demonstrated within a single species (Hulbert et al., 2002). Such data are virtually absent for invertebrates, thus the functional connection between membrane structure and permeability, on the one side, and metabolic rate and body size of invertebrates, on the other, is not known.

The present study aims to test the MPT and thus the allometry of metabolic rate and membrane lipid structure at different levels of biological organisation in an aquatic invertebrate the marine blue mussel *Mytilus edulis*. In particular, we determined the effects of body mass on heart rate and oxygen consumption rate at whole-organism, tissue and cellular levels, as well as on metabolic enzyme activities and on the lipid composition of membranes. We hypothesized that within one species the allometric scaling of metabolic rate will be pronounced at all levels, from organismal to cellular. With increasing body size, we also expected an allometric reduction in metabolic enzyme activities paralleled by an increase in the saturation level of fatty acids in membrane phospholipids. Confirming the functional link especially between metabolic scaling and membrane characteristics in invertebrates would extend the general applicability of the MPT to this vast group of animals.

MATERIALS AND METHODS

Mussels *Mytilus edulis* Linnaeus 1758 were collected at the White Sea from the population cultured close to the White Sea Biological Station Kartesh (66°20′ N, 33°40′ E) in July 2011. Water temperature at the time of collection was 12°C and salinity was 24 ppt. Mussels covered a range of soft body wet mass (M) across three orders of magnitude, between 0.012 and 18.98 g.

Mussels were washed and placed in the aquaria with aerated seawater at a constant temperature of 10°C. Two-thirds of the water volume was replaced with temperature-adjusted seawater taken from the bay on a daily basis. Additional food was not provided as we assumed that sufficient food was available through regular water exchange. Acclimation lasted 9 days. Whole-animal measurements and most of the tissue respiration measurements and sampling for lipids and fatty acids analysis were done at the White Sea Biological Station, while heart rate, tissue respiration (partly) and cellular respiration as well as enzyme activities were analysed at the Alfred Wegener Institute (AWI, Bremerhaven, Germany). In the institutional aquarium facility, mussels were kept at 12°C in separate tanks filled with aerated and filtered natural seawater from the North Sea, diluted to a salinity of 24 ppt. They were fed daily with a commercial living algal blend (DT Live Marine Phytoplankton, Coralsands, Germany). Total water exchange was performed every second day. For a consecutive study of the allometry of heart rate specimens from different size classes, *M. edulis* were collected in the German Wadden Sea (AWI station Sylt, at an environmental water temperature of 15°C and a salinity of 32 ppt). These mussels were maintained in the flow-through aquarium system with aerated and filtered natural North Sea water at 15°C and a salinity of 32 ppt.

Whole-animal respiration

Oxygen consumption rates were measured in closed respirometers of 200–500 ml volume at 10°C. Mussels were subdivided in five size groups: very small (SS, 0.046±0.005 g soft body wet mass, 15 mm length), small (S, 0.216±0.008 g, 23 mm), medium (M, 0.430±0.025 g, 30 mm), big (B, 1.327±0.092 g, 40 mm), and very big (BB, 8.186±0.447 g, >50 mm). Respirometers contained one to nine mussels depending on animal size and respirometer volume. Animals were allowed to recover from handling stress prior to closing the chambers. After 60–90 min in the respirometer, water samples were carefully drained from the chamber into air-tight bottles. Oxygen concentration was determined according to Winkler as described in Strickland and Parsons (1968). Oxygen consumption was calculated from the difference between oxygen concentration in the experimental chambers and control chambers, which were similarly exposed but contained no animals. Whole-animal mass-specific respiration rate R_{org} was expressed as μmol O_2 (g soft body wet mass)$^{-1}$ h^{-1}.

MRI recordings of the beating heart

Heart rates in mussels of S, M and B size classes (0.131±0.010, 0.841±0.075 and 3.178±0.218 g, respectively) were determined through magnetic resonance imaging (MRI) of heart motion (Lannig et al., 2008; Seo et al., 2014a). Animals classified as BB were not available for this experiment and heart rate of SS animals could not be measured because of constraints associated with the resolution of MRI hardware. All experiments were performed in a horizontal 4.7T MRI scanner with a 40 cm bore equipped with Avance III electronics. (Bruker Biospec 47/40, Bruker Biospin, Ettlingen, Germany). An 8 cm volume coil (^{1}H-birdcage resonator) was used in a gradient coil of 200 mT m^{-1} (BGU12, Bruker Biospin) for signal excitation and perception.

MRI recordings were performed on individuals exposed to air at 15°C following the approach of Seo et al. (2014a). Shell closure during air exposure was shown to have no effect on heart rate and haemolymph oxygen tension for up to 6 h in *Mytilus californianus* (Bayne et al., 1976). When submersed, however, mussels displayed spontaneous shell movements (Seo et al., 2014b) that hamper the quality of the MR images. Thus, our chosen approach guaranteed reproducibility and comparable physiological conditions as well as a minimization of movement artefacts since all mussels were completely closed during the MRI measurements. In fact, heart rates obtained in air are comparable to literature data recorded in submersed *M. edulis* [19–20 beats min^{-1} at 14°C, unknown shell length (Braby and Somero, 2006) and 13±2 beats min^{-1} at 10°C, 50–90 mm shell length (Zittier et al., 2015)]. The similarity of data sets from air-exposed and submersed mussels confirms the reliability of our experimental approach.

Individual animals were placed in a small Perspex chamber and fixed with dental wax to the bottom of the chamber (as in Bailey et al., 2003) to prevent further potential artefacts in the MR images induced by movements of the animal or by vibrations from the

Journal of Experimental Biology (2017) 220, 1423-1434 doi:10.1242/jeb.147108

gradient coils of the MRI system. The chamber was placed inside the ^{1}H-resonator in the center of the MRI scanner to obtain optimal magnetic field homogeneity. Prior to heart rate recordings, three perpendicular gradient echo MRIs were collected to check for the optimal position of the animal and for the location of the heart inside the mussel (as described in Lannig et al., 2008). Self-gated cardiac cine MRI (Bohning et al., 1990; IntraGate, Bruker Biospin, Ettlingen, Germany) was used in axial, sagittal or coronal orientations, respectively, for heart rate analysis. Parameters were as follows: sequence: IntraGateFLASH, TR=8 ms, TE 2.913 ms, matrix size: 256×256, FOV=30×30 mm, 1 mm slice thickness, flip angle 45 deg hermite of 1 ms length, scan time 2 min 13 s 72 ms for 300 images resulting in 20 cardiac frames. Usually, individual animals were inside the MRI scanner for no longer than 30–40 min, to minimize unwanted physiological changes induced from air exposure such as metabolic depression (see above; Bayne et al., 1976). Cardiac activity was monitored by repeated cine MRI recordings to exclude the influence of phases of bradycardia throughout the experiments. At constant heart rate, the last three recordings of each MRI set were used for calculations of heart rate (HR) to minimize the potential of disturbed cardiovascular circulation induced by initial handling stress inside the MRI scanner. Heart rate (beats min^{-1}) was derived from the pulsatile changes in MRI recordings (see Fig. 4) and calculated manually by counting the maxima or minima, respectively, in the signal time course derived from the cine MRIs using the IntraGate processing tool within the ParaVision software (ParaVision 5.5, Bruker Biospin, Ettlingen, Germany).

Gill tissue respiration

Acclimated mussels from SS, S, M, B and BB size groups (0.240±0.014, 0.901±0.117, 2.025±0.114, 3.612±0.100 and 10.705±0.625 g soft body wet mass, respectively) were sampled from the aquaria, weighed and transferred to a small plate with fresh seawater at 10°C. Mussels were opened while constantly covered with water and gill tissues were excised with scissors and carefully placed into the respirometer. Residual tissues were removed from each mussel, blotted dry and weighed. After the respiratory assay gill tissues were removed from the respirometers and weighed. Oxygen consumption measurements in isolated gill tissue were carried out at 10°C in closed respirometers by using the following two methods.

Respirometers (about 20 ml volume) filled with aerated and filtrated seawater contained pieces of gill tissue (M_{tissue}=40–380 mg) of one to five mussels depending on animal size classes. After an exposure period of 70–120 min, water samples were carefully drained from the chamber into air-tight bottles and oxygen concentration was determined by the Winkler method as described above. Variation in tissue masses and exposure periods was due to the fact that we tried to keep a similar ratio of $V_{respirometer}/M_{tissue}$ for all respiration recordings to ensure accurate measurements and a consistent decline of oxygen content. Since tissue pieces were weighed after the oxygen consumption measurements, tissue masses were estimated visually and exposure period decreased for larger tissue samples. Oxygen consumption was calculated from the difference between oxygen concentration in the experimental chambers and control chambers, which were exposed to the same procedure but contained no tissue samples.

At the AWI, we used needle-type oxygen microsensors (Tx-Type, PreSens, Germany) for online monitoring of oxygen consumption. Pieces of gill tissue (M_{tissue}=9–47 mg) were excised from individual animals and placed in 1 ml seawater-filled respiration chambers with inserted micro-optodes. Prior to measurements, a two-point calibration was performed at 10°C using saturated sodium sulfite solution for 0% and air-bubbled seawater for 100% air saturation. The progressive decline in oxygen concentration was monitored for 30–40 min. Drift (change in oxygen concentration recorded in a chamber without tissue) was subtracted when respiration rate was calculated.

The different methods did not affect the respiration rates (see Calculations and statistics; P=0.110, $F_{1,85}$=2.60) and data were pooled for further analysis. Tissue respiration rate (R_{gill}) was expressed as nmol O_2 (g gill tissue wet mass)$^{-1}$ min^{-1}.

Respiration of isolated gill cells

Oxygen consumption was determined in cell suspensions prepared from the gills of mussels of different sizes (S, 0.343±0.064 g; M, 2.411±0.375 g; BB, 9.341±0.765 g). Isolation of cells was performed after Lannig et al. (2010) with modifications. Briefly, 0.5–1 g of gill tissue was excised as described above, from one to 10 specimens of mussels, depending on their size. Gills were transferred to a pre-weighed Petri dish with a small portion of ice-cold isolation buffer (20 mmol l^{-1} HEPES, 325 mmol l^{-1} NaCl, 12.5 mmol l^{-1} KCl, 5 mmol l^{-1} EDTA, 750 mOsm, pH 7.5) and weighed to determine the exact tissue mass. Then the tissue was torn to small pieces with forceps, transferred to a dish with 10–15 ml isolation buffer, placed on ice on a shaker for 1 h and triturated with a plastic pipette once every 15 min. After 1 h, the rest of the tissue was filtered through 100 µm gauze washed by ice-cold isolation buffer. The resulting suspension (~15–20 ml) was centrifuged at 4°C and 800 ***g*** for 6 min. The supernatant was discarded and the pellet resuspended in 3 ml of fresh ice-cold suspension buffer (186 mmol l^{-1} NaCl, 9.13 mmol l^{-1} KCl, 12.5 mmol l^{-1} $CaCl_2$, 2.14 mmol l^{-1} $NaHCO_3$, 30 mmol l^{-1} HEPES, 46.6 mmol l^{-1} $MgCl_2$, 52.4 mmol l^{-1} $MgSO_4$, 13.6 mmol l^{-1} glucose, 750 mOsm, pH 7.5) and centrifuged at 4°C and 300 ***g*** for 12 min. The supernatant was discarded and the pellet was resuspended in 2 ml of fresh suspension buffer and centrifuged at 4°C and 250 ***g*** for 12 min. The pellet was then resuspended in 1.5 ml suspension buffer. Cell density was determined in a Fuchs–Rosenthal counting chamber and adjusted to 6×10^6 cells ml^{-1}. A cell viability of 60–70% was determined by using a standard Trypan Blue exclusion assay. Cellular respiration was determined in 1 ml water-jacketed, air-tight chambers for 30 min in three replicates using the oxygen microsensors from PreSens (see above). A two-point calibration was performed at 10°C using saturated sodium sulfite solution for 0% and air-bubbled medium for 100% air saturation. All respiration measurements were performed at 10°C and corrected for the drift of micro-optodes in the suspension buffer. Cellular respiration rate (R_{cell}) was expressed as nmol O_2 10^{-6} cells min^{-1}.

Lipid and fatty acid analyses

Lipid and fatty acid (FA) composition of tissues was determined using the facilities of the Equipment Sharing Centre of the Institute of Biology, Karelian research center of the Russian Academy of Sciences. Mussels (0.15–9.88 g soft body wet mass) acclimated to 10°C were sampled for the analyses. The mean mass in each size group was: SS, 0.168±0.012 g; S, 0.343±0.046 g; M, 1.680±0.176 g; B, 3.946±0.182 g; BB, 9.022±0.492 g. Mussels were cut open and gills were dissected, weighed, placed in a chloroform:methanol mixture (2:1, by volume) and stored at +4°C until analysis. One sample contained 0.3–0.5 g of wet gill tissue pooled from one to six similarly sized mussels. Lipids were extracted by Folch's method (Folch et al., 1957). Fractionation of total lipids was performed by thin-layer chromatography (TLC) on Silufol plates in a mixture of petroleum ether:diethyl ether:acetic acid (90:10:1, by volume). The

Journal of Experimental Biology (2017) 220, 1423-1434 doi:10.1242/jeb.147108

concentrations of membrane phospholipids, triacylglycerols and cholesterol esters were determined by the hydroxamate method (Sidorov et al., 1972). Cholesterol levels were determined by Engelbrecht's method (Engelbrecht et al., 1974). Isolated fractions of phospholipids were subjected to direct methanolysis (Tsyganov, 1971). The obtained mixtures of fatty acid methyl esters (FAME) were determined on a Crystal 5000.1 gas chromatograph (Chromatec Analytic, Russia) with a flame ionization detector using Zebron ZB-FFAP columns (50 m, 0.32 mm) (Phenomenex) and helium as a mobile phase. Fatty acids were identified by comparison with standard FAME mixture (Supelco) using Chromatec Analytic computer software. Fractional analysis of phospholipids was performed with a Stayer high performance liquid chromatograph (Akvilon) with isocratic elution and UV detector according to Arduini et al. (1996) using a Nucleosil 100-7, 250 mm silica gel column (Elsico) and acetonitrile/hexane/methanol/phosphoric acid (918:30:30:17.5, respectively by volume) as a mobile phase. The detection wavelength was 206 nm. Phospholipid fractions were identified by reference to retention times of authentic standards (Sigma Aldrich and Supelco). In the following, we assume that the phospholipids identified are major membrane components (cellular, mitochondrial, endoplasmic reticulum).

Enzyme activities

Enzyme capacities of citrate synthase (CS) and cytochrome c oxidase (COX) were determined in gill tissue of mussels of M, B and BB size groups with average soft body mass of 1.557±0.138 g, 3.034±0.203 g and 7.005±0.511 g, respectively. Animals of small size classes were not suitable for tissue sampling.

Enzyme extracts were prepared following the protocol by Windisch et al. (2011). In brief, frozen samples were homogenized in 10 volumes of buffer (20 mmol l^{-1} Tris-HCl, 1 mmol l^{-1} EDTA, 0.1% Triton X-100, pH 7.5), either directly with a glass homogenizer (small samples) or by grinding the tissue under liquid nitrogen first followed by mixing of the powdered tissue with the adequate buffer volume by use of a vortex. After Ultra Turrax treatment (3×10 s at 16,000 rpm on ice), samples were centrifuged for 10 min at 1000 ***g*** and 0°C.

Enzyme activities were measured with a microplate reader six times at 20°C. CS activity was determined following a protocol modified from Sidell et al. (1987). Assays were carried out in 75 mmol l^{-1} Tris-HCl (pH 8), 0.25 mmol l^{-1} DTNB [5,5′-dithio-bis-(2-nitrobenzoic acid)], 0.4 mmol l^{-1} acetyl-CoA and 0.4 mmol l^{-1} oxaloacetate at 412 nm. COX activity was determined after a protocol modified from Moyes et al. (1997). Homogenates (diluted 1:2) were tested in 20 mmol l^{-1} Tris-HCl (pH 8) containing 0.5% Tween 20 and 0.05 mmol l^{-1} reduced cytochrome c at 550 nm. Cytochrome c was dissolved in 20 mmol l^{-1} Tris-HCl (pH 8) and reduced by the addition of sodium dithionite, which was removed by gel filtration using a Sephadex G-25 column. Enzyme activities expressed as units (g gill tissue wet mass)$^{-1}$ were calculated using the extinction coefficients of ε_{412}=13.6 mmol^{-1} cm^{-1} for CS and ε_{550}=19.1 liters mmol^{-1} cm^{-1} for COX.

Calculations and statistics

The degree of unsaturation of phospholipids was estimated using both unsaturation index (UI) and double bond index (DBI), which were calculated as UI=ΣSFA/ΣUFA, and DBI=(% MUFA + 2 × % dienoic FA + 3 × % trienoic FA + 4 × % tetraenoic FA + 5 × % pentaenoic FA + 6 × % hexaenoic FA)/100, where FA is fatty acids; UFA, unsaturated fatty acids; MUFA, monounsaturated fatty acids; and SFA, saturated fatty acids. All allometric relationships were expressed as a power function of body mass according to the formula $Y=aM^b$, where Y is the parameter of interest, M is body mass (g soft body wet mass), a and b are the corresponding constants.

Effects of animal body mass on mussel heart rates, oxygen consumption rates, enzyme activities and lipid and fatty acid composition were estimated either by standard algorithms of regression analyses or tested using one-way ANOVA after transformation of the dependent variables. Where the assumptions to perform parametric ANOVA could not be met, Kruskal–Wallis rank ANOVA was used. To test for a possible impact of the different methods used for the measurements of tissue respiration we included the factor 'Method' as random effect in linear mixed-effects regression model. Statistical significance was tested at the P<0.05 level. All data are presented as mean values±s.e.m. unless specified otherwise.

RESULTS

Respiration rate: whole-animal, tissue and cellular levels

Whole-animal mass-specific oxygen consumption rates of *M. edulis* varied between 0.87 and 19.06 µmol O_2 (g wet mass)$^{-1}$ h^{-1}. The allometric decline of whole-animal respiration with increasing body mass was typical and highly significant (b=−0.333±0.022, P<0.0001, $F_{1,90}$=220.9, n=92) (Fig. 1). Gill tissue respiration rates varied from 28.1 to 272.9 nmol O_2 (g gill tissue wet mass)$^{-1}$ min^{-1} (mean value 118.9±41.9) and an allometric relationship failed to be significant (b=−0.056±0.031, P=0.075, $F_{1,85}$=3.24, n=87) (Fig. 2). The average respiration rate in gills of the smallest mussels (SS group) was ∼50% higher than the average obtained in the other size groups; however, data variability was high and this pattern was not significant (Tukey HSD test, P=0.188). Cellular respiration varied markedly and demonstrated a decrease with increasing mussel body mass in the studied size ranges (Fig. 3); however, the power regression was nearly significant (b=−0.098±0.050, P=0.063, $F_{1,20}$=9.87, n=22). On average, gill cells consumed 0.095±0.045 nmol O_2 10^{-6} cells min^{-1}.

Heart rate

Fig. 4 presents examples of axial cine MR images of a small mussel in comparison to a big mussel and their respective time courses of heart rates. The heart (H) is located on the left side near the shell of the MR images. The bright spots arose from hemolymph flow through vessels (V) and fluid through the cavities (C, only visible in the big mussel). Time courses present cardiac raw data after around

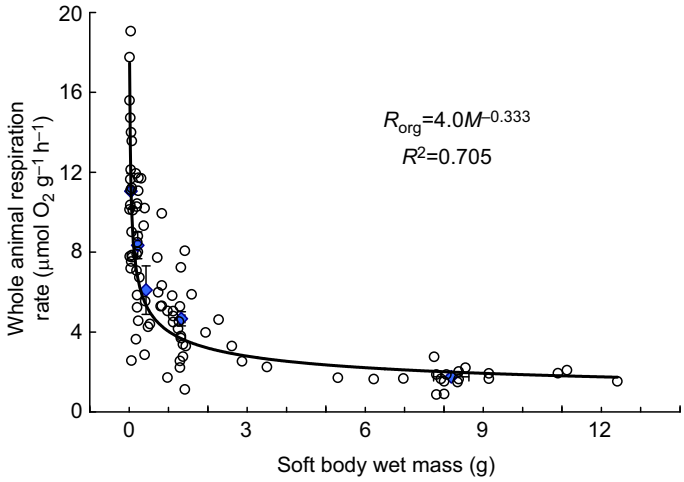

Fig. 1. Whole-animal respiration as a function of body mass. Blue points represent the mean±s.e.m. values for different size groups (n=92, P<0.0001).

Journal of Experimental Biology (2017) 220, 1423-1434 doi:10.1242/jeb.147108

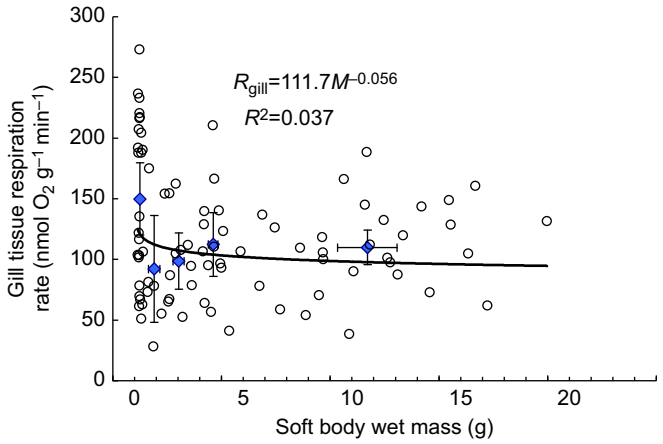

Fig. 2. Gill tissue respiration as a function of body mass. Blue data points represent the mean±s.e.m. values for different size groups (n=87, P=0.075).

60 to 130 s of the cine MRI recordings. The difference in frequency and signal-to-noise ratio results from different heart rates and amplitudes between small and big mussels. Indeed, heart rate showed a pronounced allometric decline from more than 25 beats per minute in small animals to less than 10 beats per minute in big mussels. An allometric exponent b=−0.203±0.041 was highly significant (P<0.0001, $F_{1,21}$=24.08, n=23) (Fig. 5).

Enzyme activities

CS and COX activities in gill tissue varied in a relatively narrow range between 2.9–4.8 and 8.6–16.1 U (g gill tissue wet mass)$^{-1}$, respectively, and were positively correlated with each other (Spearman R=0.636, n=15, P<0.05). Despite a weak allometric trend, the decline of activities of both enzymes in gill tissue with increasing mussel body mass was not significant (Fig. 6A,B), in line with small changes in tissue and cellular oxygen consumption rates.

Lipid composition and fatty acid profile

Lipids comprised 10–13% of gill tissue dry mass with the absolute major components being membrane structural lipids – phospholipids and cholesterol (Table 1). Storage lipids (triacylglycerol and cholesterol esters) represented only ∼5–6% of total lipid content in gill tissue of all size classes. Phospholipids in mussel gill tissue comprised mostly phosphatidyl choline (PC, ∼83% of all phospholipids) with phosphatidyl ethanolamine (PE), phosphatidyl serine (PS), phosphatidyl inositol (PI), lysophosphatidyl choline (LPC) and sphingomyelin (SM) as minor constituents (Table 1). Total lipid (TL) content as well as the phospholipid (PL) fraction declined significantly in gills with increasing body mass (b=−0.062±0.014, P<0.0001, $F_{1,27}$=21.03, n=29 for TL and b=−0.063±0.014, P<0.001, $F_{1,26}$=20.32, n=28 for PL) (Fig. 7A). The overall reduction of membrane structural lipids in the largest mussels (BB size group) compared with the smallest ones (SS group) was ∼25%, while in the individual lipid classes, such as PI, PE and PC, the decline was even more pronounced, resulting in up to a 50% reduction (Table 1, Fig. 7B). Storage lipids of gill tissue showed no significant allometric changes. A significant positive correlation was observed between the concentrations of cholesterol and phospholipids (Spearman R=0.601, n=29, P<0.001).

The profile of fatty acids (% of total fatty acids) in phospholipids of gill tissue is provided in Table 2. On average, the FA pool contained 43.1% PUFA (polyunsaturated fatty acids), 21.8% MUFA, 20.5% SFA and 14.6% NMIFA (non-methylene interrupted fatty acids), with no trends in % composition with body size. Some fatty acids, specifically docosahexaenoic acid (DHA, 22:6n-3), eicosapentaenoic acid (EPA, 20:5n-3), palmitic acid (16:0), as well as 20 and 22 NMIFA, dominated, covering >50% of the total pool. The concentrations of seven fatty acids showed significant allometric decreases or increases in gill phospholipids with increasing body size (Fig. 8). Concentrations of two major long-chain PUFA changed in opposite directions: DHA declined (albeit not significantly, P=0.099) while its precursor, EPA, increased (Fig. 8C) with increasing body size. Similarly, a decrease of oleic (18:1n-9), α-linolenic (18:3n-3), and docosapentaenoic (22:5n-6) acids was accompanied by an accumulation of odd-chain saturated fatty acid (15:0), monoenic 20:1n-11, and arachidonic (20:4n-6) acids as mussels became larger (Fig. 8). The amount of PUFA, the ratio of PUFA over SFA and the degree of unsaturation (UI and DBI) did not vary with body mass.

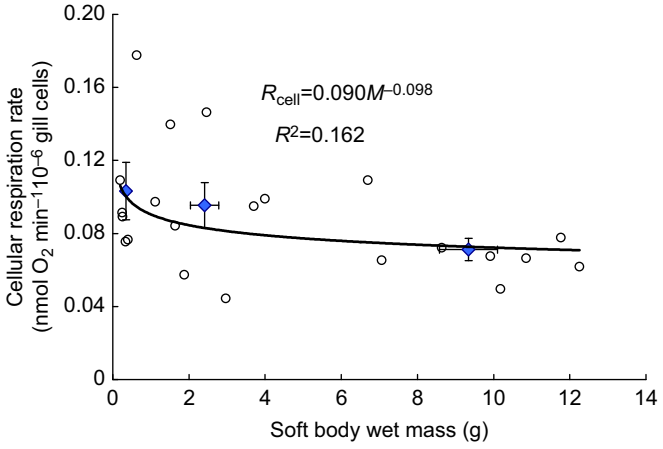

Fig. 3. Cellular respiration of isolated gill cells as a function of body mass. Blue data points represent the mean±s.e.m. values for different size groups (n=22, P=0.063).

DISCUSSION

We tested the MPT at several levels of biological organisation from subcellular to organismal functions such as whole-animal respiration and heart rate. Our data support the suggested hypothesis only partly. At the whole-organism level, metabolic and heart rates of the blue mussel clearly followed allometric patterns, with exponents of −0.333 and of −0.203, respectively. The latter findings already indicate a role for cardiac activity in following the metabolic scaling and thereby contributing to an allometric pattern at the whole-organism level. In mammals and fish, heart size and therefore stroke volume increase proportionally to body mass (Prothero, 1979; Farrell et al., 1988). Although not quantified because of the limited resolution of our MR scanner, the cardiac images of *M. edulis* also indicate rising stroke volume with increasing animal size (e.g. brighter and bigger spots in larger mussels). Larger hearts gain efficiency and the fractional energy cost of cardio-circulation decreases with increasing body size.

Our findings show that metabolic allometry although well expressed at the whole-organism level was much less pronounced at tissue and cellular levels. Furthermore, we found no body mass-related changes in the fatty acid unsaturation of membrane phospholipids. We propose several reasons that might explain the relatively poor support of the MPT paradigm in our results: (1) MPT was proposed for interspecific comparisons whereas we tested it

Journal of Experimental Biology (2017) 220, 1423-1434 doi:10.1242/jeb.147108

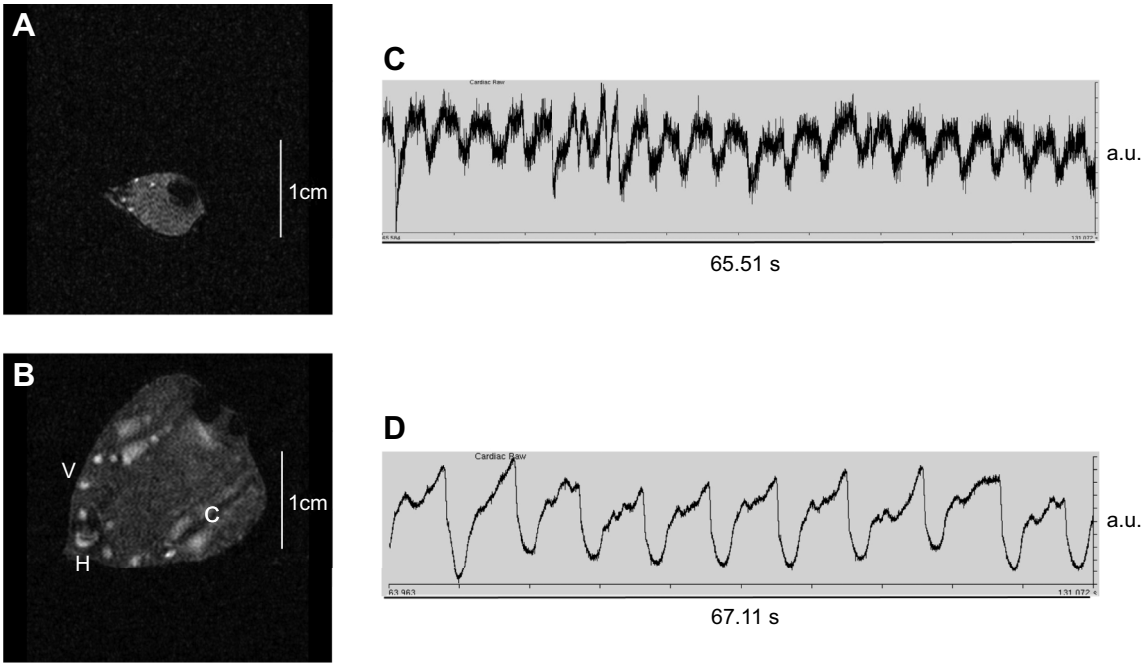

Fig. 4. Axial MR images of two individual *M. edulis* of different size recorded with cine MRI. (A,B) Small mussel 20 mm in length (A) and large mussel 50 mm in length (B). The heart (H), hemolymph in vessels (V) and fluid through the cavities (C) is indicated in B. (C,D) Cardiac signal changes over time; used to calculate the heart rate. The larger mussel (D) shows a higher signal-to-noise ratio but lower frequency over time, indicating a lower heart rate compared with the small animal (C).

within a single species; (2) whole-animal (systemic) allometry may not necessarily extend to the sub-organismal level; (3) MPT was proposed for endotherms whereas we tested it for an ectotherm. We also consider to what extent an allometric decline in tissue phospholipid content can support metabolic allometry.

Interspecific versus intraspecific scaling of MR

Metabolic allometry at the interspecific level is widely accepted because the body size range is large and data allow generalizations. Most theories, including MPT, deal with between-taxa scaling (see Introduction). However Kleiber's Law also holds true at the intraspecific level (based on classical work by Rubner, 1883 on dogs; see also Bokma, 2004; Kerkhoff, 2012; Konarzewski and Książek, 2013; Carey et al., 2013). Interspecific comparisons may include taxonomically diverse groups, such as insects and mammals. However, including closely related congeneric species or hybrids may bring such comparisons closer to those at the intraspecific level. Intraspecific allometry is routinely considered in clinical pharmacology and medicine (e.g. Anderson and Holford, 2008; Cella et al., 2010) and always considered in measurements of physiological rates when the raw data obtained are corrected for a standard body mass. Hulbert (2010) noted that the MPT may not explain intraspecific scaling because variations in metabolic rate within a species may not be associated with differences in membrane fatty acid composition. However, similar constraints should apply to both intra- and interspecific comparisons and a universal theory should be able to explain allometric patterns at both inter- and intraspecific levels. Such theory, however, may require consideration of various inter-dependent components across levels of biological organisation (see below).

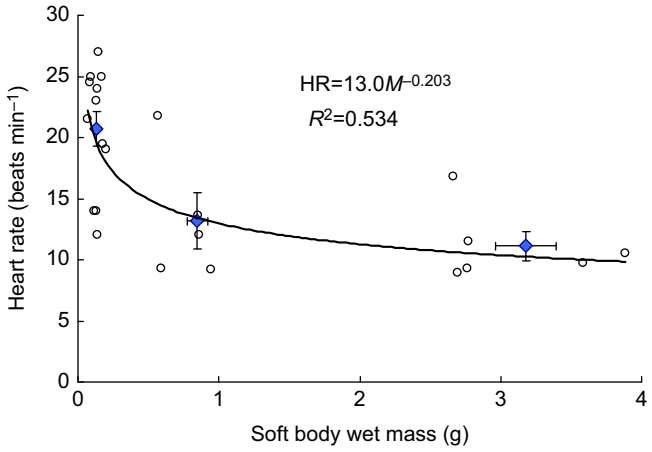

Fig. 5. Heart rate as a function of body mass. Blue data points represent the mean±s.e.m. values for different size groups (n=23, P<0.0001).

According to the MPT, it is the structure of membranes and their efficiency in maintaining transmembrane ion gradients in cells and mitochondria that change with body size and determines metabolic rate and its allometry (Hulbert and Else, 1999, 2000; Hulbert, 2007). Smaller mammals and their most metabolically active tissues contain more polyunsaturated fatty acids in cell and mitochondrial membranes compared with larger animals. The key component was found to be docosahexaenoic acid (22:6n-3), which showed a pronounced decline with body size in mammals and birds (Gudbjarnason et al., 1978; Couture and Hulbert, 1995a; Hulbert and Else, 2004). However, we did not find any allometric pattern in the degree of unsaturation of membrane fatty acids in gill tissue from mussels of different sizes. DHA declined somewhat but this decline was insignificant. In gill phospholipids, constant ratios of n-3/n-6 PUFA and SFA/PUFA as well as constant unsaturation and double bond indices in different size groups apparently provide relatively stable activities of membrane-bound enzymes and hence size-independent respiration rates in gill tissue and cellular preparations. Since the synthesis pathway for PUFA is practically absent or

Journal of Experimental Biology (2017) 220, 1423-1434 doi:10.1242/jeb.147108

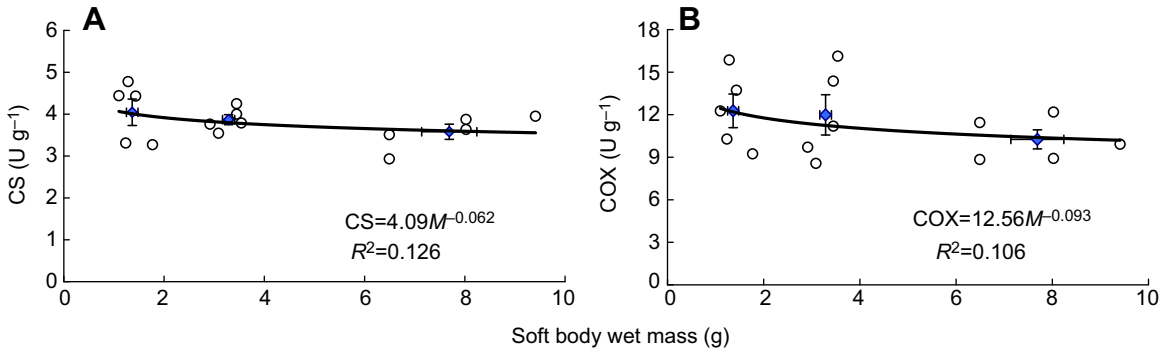

Fig. 6. Activity of citrate synthase and cytochrome C oxidase in mussel gill tissues as a function of body mass. Activity of (A) citrate synthase (CS; n=15, P=0.194) and (B) cytochrome C oxidase (COX; n=15, P=0.237) measured in units (g gill tissue wet mass)$^{-1}$. Blue data points represent the mean±s.e.m. values for different size groups.

greatly reduced in bivalves (De Moreno et al., 1976, 1977), PUFA are taken up via the food. This may imply that the composition of essential fatty acids in membrane phospholipids is strongly regulated. Any differences in the fatty acid profile of the studied size groups of mussels may thus be associated with diet composition and the selective assimilation of the fatty acids by mussels.

In large mollusks, a declining proportion of phytoplanktonic FAs (Viso and Marty, 1993), such as α-linolenic 18:3n-3, docosapentaenoic 22:5n-6 acids (Fig. 8B,D) and oleic 18:1n-9 and docosahexaenoic 22:6n-3 acids (dinoflagellate markers) (Fig. 8A,C), together with a concomitant increase in eicosapentaenoic 20:5n-3 acid (Fig. 8C) (a marker of diatoms) and arachidonic 20:4n-6 acid (zooplankton marker), probably indicates the selective consumption of diatoms and zooplankton (Rouillon and Navarro, 2003). An increase in the content of arachidonic acid may be related to both the selective uptake of zooplankton and the additional synthesis of this FA from its precursor – linoleic 18:2n-6 acid in the gills of large mussels (Newton et al., 2013). The accumulation of odd-chain saturated fatty acid (15:0), a marker of bacteria from detritus (Volkman et al., 1980) and a zooplankton 20:1n-11 monoenic acid (Sargent and Falk-Petersen, 1988), in the gills of mussels probably indicates a wider dietary spectrum of larger mussels, as well as low turnover rates of these minor fatty acids. None of these alterations comprises a large enough shift in lipid unsaturation to support a change in metabolic rate.

MPT sets out to explain the differences in metabolic rate between endotherms of different sizes (Hulbert, 2007) and between endo- and ectotherms (Mitchell et al., 2007), i.e. it works at the interspecific level. A recent study on 12 closely related species of cypriniform fish suggested that it also works at an intraspecific level (Gonzalez et al., 2015). At a rather narrow genetic scale, the observed allometric changes in membrane composition may thus be based on genetic cues in line with the effects of size. Some publications demonstrate a within-species ontogenetic shift from less to more saturated fatty acids in skeletal muscle membranes (but not in brain) of turkey *Meleagris gallopavo* (Szabó et al., 2006) and Weddell seal *Leptonychotes weddellii* (Trumble and Kanatous, 2012). However, basal metabolic rate may not always be affected; for example, the basal metabolic rate and fatty acid composition of membranes were unrelated in mice selected for highly varied basal metabolic rate (Brzęk et al., 2007; Haggerty et al., 2008). The present study on an aquatic ectotherm also does not support the predictions of the MPT and may thus provide further evidence that the model is less important at the intraspecific level (Hulbert, 2010; Konarzewski and Książek, 2013).

Metabolic scaling at tissue and cellular levels

The dependence of metabolic rate on the body size of mussels became progressively weaker at suborganismal tissue and cellular levels. This was unexpected because an allometric decline of tissue and cellular metabolic rate was reported in some, mostly

Table 1. Proportion of total lipids and lipid class in gill tissue of mussels of different size groups

	Size group				
Lipid class	SS (n=4)	S (n=4)	M (n=5)	B (n=4)	BB (n=5)
Total lipids (TL), % of dry tissue mass	13.31±0.71^{a}	13.26±0.40^{a}	11.84±0.45^{a,b}	11.88±0.43^{a,b}	10.40±0.37^{b}
Phospholipids (PL), % of dry tissue mass	8.21±0.23^{a}	7.89±023^{a,b}	7.31±0.21^{a,b}	7.60±0.21^{a,b}	5.97±0.28^{b}
TAG (% of dry tissue mass)	0.59±0.25	0.26±0.18	0.24±0.09	0.28±0.13	0.21±0.04
CE (% of dry tissue mass)	0.16±0.05	0.42±0.13	0.40±0.11	0.26±0.08	0.33±0.08
Cholesterol (% of dry tissue mass)	4.35±0.49	4.68±0.27	3.89±0.22	3.75±0.28	3.90±0.19
Cholesterol/PL	0.53±0.05	0.59±.0.3	0.53±0.03	0.49±0.04	0.66±0.03
PI (% of phospholipids)	0.20±0.03	0.16±0.05	0.14±0.03	0.10±0.02	0.09±0.02
PS (% of phospholipids)	0.25±0.05	0.17±0.01	0.14±0.03	0.12±0.02	0.14±0.02
PE (% of phospholipids)	0.55±0.10	0.47±0.05	0.46±0.04	0.37±0.08	0.32±0.04
PC (% of phospholipids)	6.46±0.20^{a}	6.32±0.27^{a,b}	6.17±0.22^{a,b}	6.58±0.23^{a,b}	5.05±0.20^{b}
LPC (% of phospholipids)	0.06±0.01	0.02±0.005	0.04±0.004	0.05±0.01	0.04±0.004
SP (% of phospholipids)	0.04±0.02	0.01±0.00	0.01±0.004	0.02±0.01	0.02±0.004
Unidentified lipids	0.49±0.08	0.46±0.08	0.36±0.05	0.35±0.03	0.31±0.08
PE/PC	0.09±0.02	0.08±0.01	0.07±0.01	0.06±0.02	0.06±0.01

Means±s.e.m. are presented. For each trait size, groups annotated with the same superscript letter or without these marks do not differ significantly (P<0.05). TAG, triacylglycerol; CE, cholesterol ester; PI, phosphatidyl inositol; PS, phosphatidyl serine; PE, phosphatidyl ethanolamine; PC, phosphatidyl choline; LPC, lysophosphatidyl choline; SP, sphingomyelin.

Journal of Experimental Biology (2017) 220, 1423-1434 doi:10.1242/jeb.147108

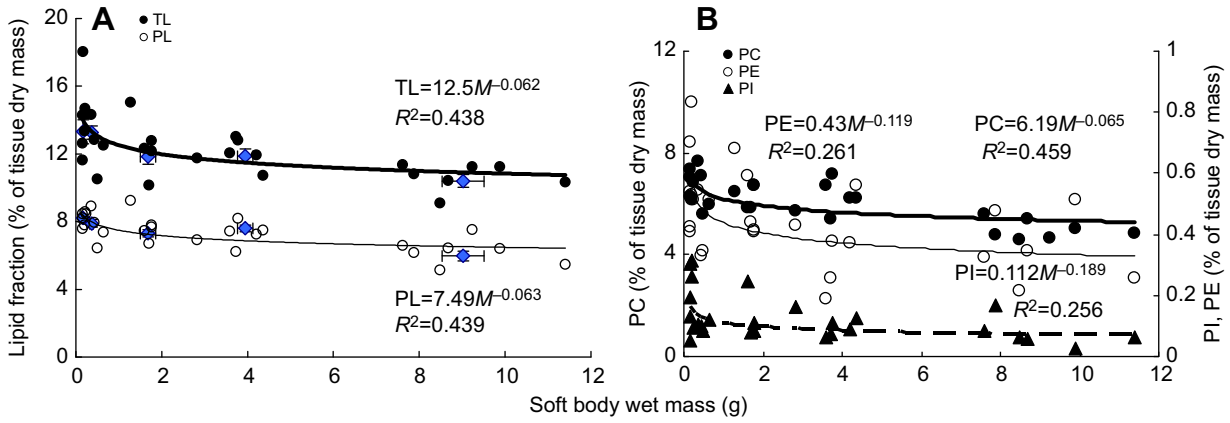

Fig. 7. Lipid content as a function of body size. Total lipids and phospholipid content (A) and fraction of phospholipids of different classes (B) (n=28, P<0.01). Regressions of different phospholipids on soft body mass are: PC=6.19$M^{-0.065}$, R^2=0.459, P<0.0001; PE=0.43$M^{-0.119}$, R^2=0.261, P<0.01; PI=0.112$M^{-0.189}$, R^2=0.256, P<0.01. Blue data points in A represent the average values for different size groups.

endothermic species. Some studies in mammalian liver, spleen and lung revealed very similar tissue-specific cell sizes between small and large animals, whereas respiration of tissue slices and cells scaled with body mass with the exponent ranging from −0.21 to −0.07 dependent on tissue type (Couture and Hulbert, 1995b; Porter and Brand, 1995; see Porter, 2001 for review). The lower cellular metabolic rate found in larger mammals was explained by a decrease in ATP turnover due to a decline of Na^+/K^+-ATPase activity (Couture and Hulbert, 1995b), associated with either lower mitochondrial density (mitochondrial membrane surface area, Else and Hulbert, 1985) and/or increased mitochondrial efficiency. Proton leak in mammalian mitochondria scales with animal body mass with an exponent of −0.13 (Porter et al., 1996). Allometric changes in mitochondrial volume and membrane surface area were found also in fish (Burpee et al., 2010) and the bivalve *Aequipecten opercilaris* (Philipp et al., 2008). However, our data poorly support body size-related mitochondrial changes in mussels, at least in the gills. In line with a poor body mass-related metabolic decline at tissue and cellular level in gills, both CS and COX activities in this tissue showed a weak allometric decrease (b=−0.06 and −0.09, respectively) albeit not statistically significant. The body mass-related decrease in phospholipids observed in gills may thus be only partially explained by the respective changes in mitochondrial density. Metabolic allometry in mammalian cells was detected only *in vivo* and partially or completely dissipates in *in vitro* cell cultures (West et al., 2002; Glazier, 2015). The authors viewed this observation as a corroboration of the crucial role of organismal functions, such as supply networks or regulatory processes, for maintaining the allometry of metabolic rate.

Besides potential changes in mitochondrial density (and their membranes) the observed decline in phospholipid contents in the gills would also be found if larger mussels had larger cells. In this case, the number of cells per gramme of tissue would be smaller and the mass-specific concentration of membrane components (and therefore phospholipids) would also be less because of surface-to-volume allometry. A decreasing phospholipid content in larger cells implies reduced transmembrane transport activity and thus lower metabolic rate per unit body mass, but not per constant number of cells. This is in line with our observation of reduced allometry of cellular respiration in mussels. Johnston et al. (2003) found a strong positive correlation between body size and maximum muscle fibre diameter and a body size-related decrease in muscle fibre number in several fish species. This allowed the authors to suggest an 'optimal fibre size hypothesis', which explains the allometry of muscle fibre diameter in relation to body size through a trade-off between avoiding diffusion limitations and the need to minimize the costs of ion pumping across membranes (Johnston et al., 2004). This hypothesis has been experimentally supported for fish and crustaceans by Jimenez et al. (2011, 2013), who showed that bigger specimens have larger muscle fibres than smaller ones, and that the Na^+/K^+-ATPase activity as well as the energetic cost of its function is lower in larger cells because of the reduced surface area to volume ratio. An inverse relationship between cell size and animal metabolic rate was found in intraspecific studies of a few species, such as mice (Konarzewski and Książek, 2013) and fish (Maciak et al., 2011; Zhang et al., 2014). Interspecific comparisons in mammals and birds showed that cell size, although positively correlated with animal body mass, had an exponent coefficient that was too low to explain metabolic scaling in the endotherms (Kozłowski et al., 2010; White and Kearney, 2013). It may, however, contribute more prominently to allometric scaling in the mollusk.

Ectotherms versus endotherms

Hulbert et al. (2002) analysed hepatocyte respiration in 16 ectothermic species in relation to body mass. Data variability was enormous and the regression was not significant (P=0.077), but the slope was very similar to that of isolated mammalian hepatocyte respiration rates in relation to body mass (−0.191 and −0.178, respectively). An allometric decline of ATP turnover rate in muscle cells was also recorded in fish (Jimenez et al., 2011, 2013). These observations suggest that cellular maintenance costs may similarly depend on body size in vertebrate endo- and ectotherms. At the same time, mitochondrial functions in endo- and ectotherms scale differently with body size. Thus, in vertebrate ectotherms (lizards and crocodiles), unlike in mammals, an allometry of mitochondrial proton leak was not found (Hulbert et al., 2002). Similarly, the respiration rates of fish mitochondrial isolates did not show an allometric pattern (Burpee et al., 2010).

Savage et al. (2007) explored the quantitative relationships between animal body mass and cellular size, number and metabolic rate. They analyzed data published on 18 cell types in mammals ranging in size from mice to elephants. It appeared that in quickly dividing cells (most studied cell types) average cell size remained constant, whereas average *in vivo* cellular metabolic rate per unit mass of cells declined with increasing body mass$^{-0.25}$. In contrast, for slowly dividing cells like neurons and adipocytes, cell size

Journal of Experimental Biology (2017) 220, 1423-1434 doi:10.1242/jeb.147108

Table 2. Fatty acid composition (% of total fatty acids) of gill tissue phospholipids in mussels from different size groups

	Size group				
Fatty acid	SS (*n*=4)	S (*n*=4)	M (*n*=5)	B (*n*=4)	BB (*n*=5)
12:0	0.06±0.02	0.03±0.00	0.05±0.01	0.06±0.01	0.04±0.01
14:0	1.23±0.10	1.02±0.17	1.24±0.19	1.2±0.09	1.02±0.04
15:0	0.55±0.03^{a}	0.48±0.05^{a}	0.58±0.04^{a}	0.62±0.06^{a}	0.71±0.04^{b}
16:0	13.3±0.20	13.06±0.37	13.9±0.31	13.63±0.32	13.63±0.63
17:0	0.56±0.02	0.51±0.03	0.51±0.02	0.58±0.03	0.65±0.03
18:0	3.16±0.01	3.01±0.10	3.23±0.04	3.14±0.17	3.39±0.20
20:0	0.13±0.00	0.06±0.01	0.22±0.08	0.11±0.01	0.11±0.01
22:0	1.73±0.39	0.65±0.30	1.87±0.51	1.84±0.59	1.68±0.48
24:0	0.14±0.02	0.13±0.04	0.3±0.15	0.3±0.09	0.1±0.02
Σ SFA	20.86±0.27	18.96±0.54	21.9±0.82	21.48±0.27	21.32±0.37
14:1	0.78±0.36	0.38±0.10	0.45±0.17	0.42±0.11	0.35±0.05
15:1	0.28±0.08	0.1±0.04	0.13±0.04	0.19±0.06	0.17±0.03
16:1(n-11)	0.39±0.01	0.38±0.04	0.38±0.02	0.38±0.02	0.43±0.02
16:1(n-9)	0.4±0.13	0.34±0.04	0.32±0.07	0.46±0.01	0.35±0.08
16:1(n-7)	4.61±0.57	4.99±0.22	5.39±0.37	3.67±0.88	4.58±0.32
16:1(n-5)	0.09±0.05	0.06±0.02	0.08±0.02	0.03±0.01	0.05±0.01
17:1	3.15±0.96	0.86±0.17	1.43±0.21	4.1±1.03	1.39±0.30
18:1(n-11)	0.64±0.09	0.8±0.08	0.8±0.09	0.61±0.13	0.93±0.06
18:1(n-9)	3.6±0.33	2.37±0.38	2.86±0.69	2.75±0.25	1.99±0.21
18:1(n-7)	1.94±0.05	1.76±0.05	1.83±0.07	1.68±0.07	1.92±0.07
18:1(n-5)	0.08±0.01	0.11±0.00	0.13±0.01	0.12±0.02	0.09±0.01
20:1(n-11)	0.84±0.13^{a}	0.8±0.06^{a}	1.11±0.07^{b}	1.07±0.28^{a,b}	1.19±0.06^{b}
20:1(n-9)	2.94±0.41	2.93±0.12	3.08±0.10	3.33±0.28	3.12±0.21
20:1(n-7)	0.47±0.03	0.55±0.02	0.58±0.06	0.87±0.27	0.63±0.04
22:1(n-9)	0.6±0.08	0.2±0.05	0.37±0.09	0.51±0.15	0.24±0.07
22:1(n-7)	0.13±0.01	0.09±0.02	0.22±0.09	0.13±0.03	0.06±0.01
24:1(n-9)	0.15±0.03	0.22±0.10	0.18±0.05	0.29±0.04	0.09±0.02
Σ MUFA	21.07±1.10	16.95±0.60	19.32±0.39	20.61±0.35	17.57±0.32
16:3(n-3)	5.58±0.78	6.84±0.16	5.48±0.29	4.9±0.44	5.93±0.34
16:4(n-3)	0.06±0.00	0.07±0.01	0.1±0.02	0.06±0.01	0.09±0.01
18:3(n-3)	0.6±0.14^{a}	0.47±0.04^{b}	0.37±0.03^{b}	0.39±0.05^{b}	0.34±0.03^{b}
18:4(n-3)	0.61±0.08	0.77±0.04	0.69±0.04	0.68±0.10	0.92±0.07
20:3(n-3)	0.08±0.02	0.08±0.02	0.12±0.05	0.1±0.02	0.07±0.01
20:4(n-3)	0.1±0.03	0.06±0.01	0.15±0.04	0.07±0.03	0.07±0.01
20:5(n-3)	9.34±0.36^{a}	10.01±0.34^{b}	9.57±0.49^{b}	10.9±0.10^{b,c}	11.65±0.40^{c}
22:5(n-3)	1.07±0.06	1.23±0.03	1.51±0.46	1.03±0.23	1.16±0.01
22:6(n-3)	18.04±0.20^{a,b}	20.01±0.44^{a}	17.51±0.66^{a,b}	17.05±0.50^{b}	17.22±0.30^{a,b}
Σ n-3 PUFA	35.48±1.06	39.52±0.43	35.5±0.61	35.19±0.92	37.45±0.63
16:2(n-6)	0.38±0.05	0.47±0.02	0.37±0.03	0.36±0.05	0.48±0.04
18:2(n-6)	1.25±0.07	1.37±0.12	1.39±0.05	1.26±0.06	1.25±0.09
18:3(n-6)	0.05±0.01	0.06±0.01	0.08±0.02	0.06±0.01	0.05±0.01
20:2(n-6)	0.55±0.07	0.58±0.03	0.62±0.06	0.43±0.06	0.53±0.04
20:4(n-6)	3.24±0.17	3.88±0.18	3.84±0.38	3.79±0.20	4.25±0.16
22:3(n-6)	0.14±0.03	0.16±0.01	0.17±0.02	0.18±0.05	0.13±0.02
22:4(n-6)	0.4±0.06^{a}	0.48±0.06^{a}	0.42±0.05^{a,b}	0.4±0.03^{a,b}	0.45±0.03^{b}
22:5(n-6)	0.66±0.04^{a}	0.61±0.06^{a,b}	0.48±0.03^{b,c}	0.52±0.04^{c}	0.42±0.03^{c}
Σ n-6 PUFA	6.68±0.17	7.61±0.13	7.37±0.44	6.99±0.17	7.57±0.20
20NMIFA	7.19±0.21	7.27±0.27	6.66±0.41	6.78±0.61	6.72±0.14
22NMIFA	7.73±0.25	8.7±0.43	7.7±0.29	7.63±0.40	8.67±0.32
Σ NMIFA	14.92±0.12	15.97±0.66	14.36±0.65	14.41±0.66	15.39±0.40
Σ PUFA	42.16±0.94	47.13±0.48	42.87±0.48	42.18±0.75	45.01±0.69
SFA/PUFA	0.50±0.01	0.40±0.02	0.51±0.02	0.51±0.01	0.47±0.02
n-3/n-6	5.33±0.27	5.2±0.10	4.9±0.34	5.05±0.26	4.96±0.15
Σ UFA	78.16±0.17	80.06±0.55	76.56±0.50	77.20±0.77	77.97±0.34
UI	0.27±0.00	0.24±0.01	0.29±0.01	0.28±0.01	0.27±0.01
DBI	2.56±0.03	2.77±0.03	2.55±0.03	2.55±0.03	2.65±0.02

Values are means±s.e.m. For each trait size, groups annotated with the same superscript letter or without these marks do not differ significantly (P<0.05). SFA, saturated fatty acids; UFA, unsaturated fatty acids; MUFA, monounsaturated fatty acids; PUFA, polyunsaturated fatty acids; NMIFA, non-methylene interrupted fatty acids; UI, unsaturation index; DBI, double bond index.

correlated positively with body size while cellular metabolic rate per unit mass of cells was more or less constant with increasing body mass. On average, these patterns should lead to a decrease in mass-specific tissue metabolic rate. However, more experimental evidence is needed before final conclusions can be drawn.

The type of allometry found in slowly dividing mammalian cells is similar to the pattern that we observed in mussels. Thus, the cellular metabolic rate did not depend significantly on the body mass of mollusks, while the decline of membrane lipids (phospholipids) in bigger animals suggests a reduction in the

Journal of Experimental Biology (2017) 220, 1423-1434 doi:10.1242/jeb.147108

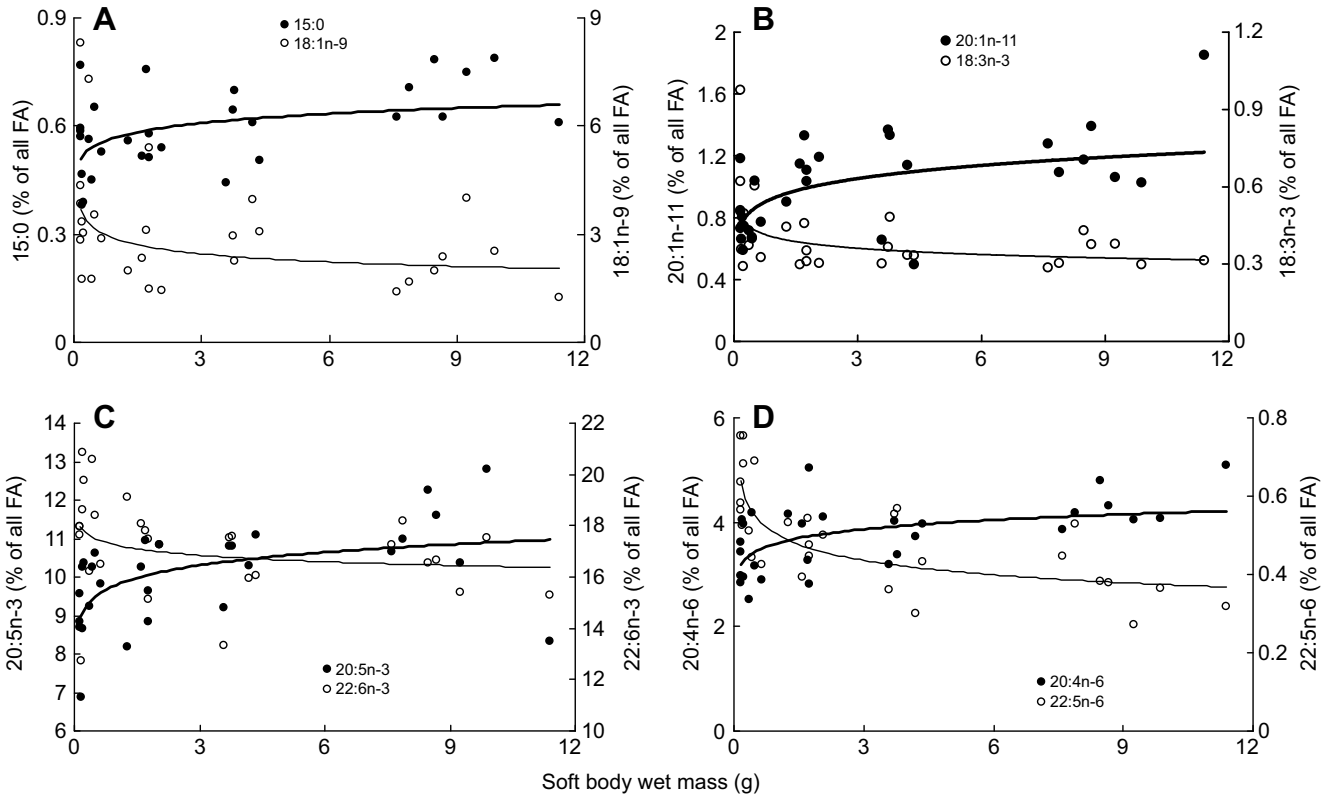

Fig. 8. Fraction of fatty acids in gill tissue as a function of body mass. Regressions of FA on soft body mass: (A) [15:0]=0.57$M^{0.062}$, R^2=0.241, P=0.070; [18:1n-9]=2.85$M^{-0.140}$, R^2=0.202, P=0.016; (B) [20:1n-11]=0.93$M^{0.110}$, R^2=0.306, P=0.002; [18:3n-3]=0.40$M^{-0.106}$, R^2=0.330, P=0.001; (C) [20:5n-3]=9.79$M^{0.048}$, R^2=0.293, P<0.01; [22:6n-3]=17.25W$^{-0.022}$, R^2=0.097, P=0.099; (D) [20:4n-6]=3.60$M^{0.065}$, R^2=0.295, P=0.029; [22:5n-6]=0.50$M^{-0.130}$, R^2=0.558, P<0.001.

tissue content of membranes, possibly as a result of increased cell size. We did not find any significant shifts in the level of FA unsaturation in relation to mussel body mass – exactly as in slowly proliferating neural brain tissue of endotherms (see Hulbert and Else, 2000; Szabó et al., 2006). At the tissue and cellular level, we studied only gills, which are composed of a combination of tissues – epithelia of several types and connective tissue. One might argue that the poor metabolic allometry recorded at the sub-organismal level in mussels is a specific feature of gills, similar to slowly proliferating neural tissues in mammals. This reasoning cannot be excluded, although it appears unlikely: the metabolic activity, proliferation and apoptosis rates in gills are among the highest found among tissue types of bivalve mollusks (Strahl and Abele, 2010).

Conclusions

Metabolic allometry in the marine mussel *Mytilus edulis* remains insufficiently explained by the MPT. Allometric patterns at sub-organismal levels of biological organization are less expressed than in mammalian systems. Allometric changes of respiration and metabolic enzymes activities in gill tissue and gill cells were poor; fatty acid unsaturation of membranes was basically independent of animal size. However, the organismal (systemic) functions and processes such as heart rate and whole-animal metabolic rate as well as phospholipid contents showed a mass-related decline. It is thus conceivable that most of the metabolic allometry observed at the whole-animal level in mussels is determined by functions at the organismal level. These whole-organism patterns may be supported by energy savings associated with growing cell size but not by structural changes in gill membranes. Hulbert et al. (2002) also reported a lack of allometry in liver phospholipid acyl composition, hepatocyte respiration rate as well as in mitochondrial proton leak in ectothermic crocodiles compared with mammals. The authors suggested that the studied species of reptiles represented a special case or there was an experimental error. However, our data support the cited study and indicate that metabolic allometry in ectotherms may be maintained through mechanisms that rely less on MPT-associated mechanisms than those in mammals and birds (see also Gonzalez et al., 2015). This may differentiate the applicability of the MPT. Further studies on cellular metabolic allometry in ectotherms are needed as well as on the allometry of cell size and cell division rates to enhance our knowledge of the relationship between metabolic rate and body size.

Acknowledgements

We thank Felizitas Daemann and Christian Buschbaum for providing us with *Mytilus edulis* from the North Sea, Olga Vozniak, Daria Martynova and Anette Tillmann, who helped us with respiration and enzyme measurements.

Competing interests

The authors declare no competing or financial interests.

Author contributions

A.S. conceived and designed the experiments; A.S., N.F., T.R., C.B. and G.L. performed the experiments and measurements; A.S. performed statistical analyses; A.S. H.-O.P., N.F., C.B. and G.L. drafted and revised the manuscript. All authors approved the final version of the manuscript.

Funding

The study was supported by the Hanse-Wissenschaftskolleg (Delmenhorst, Germany) to A.S., the Russian Foundation for Basic Research (10-04-00316 and 14-04-00466) and by the research program 'Polar regions and coasts in a changing

Earth system' (PACES) from the Alfred Wegener Institute Helmholtz Centre for Polar and Marine Research.

References

Anderson, B. J. and Holford, N. H. G. (2008). Mechanism-based concepts of size and maturity in pharmacokinetics. *Annu. Rev. Pharmacol. Toxicol.* **48**, 303-332.

Arduini, A., Peschechera, A., Dottori, S., Sciarroni, A. F., Serafini, F. and Calvani, M. (1996). High performance liquid chromatography of long-chain acylcarnitine and phospholipids in fatty acid turnover studies. *J. Lipid Res.* **37**, 684-689.

Bailey, D. M., Peck, L. S., Bock, C. and Pörtner, H.-O. (2003). High-energy phosphate metabolism during exercise and recovery in temperate and Antarctic scallops: an in vivo ^{31}P-NMR study. *Physiol. Biochem. Zool.* **76**, 622-633.

Bayne, B. L., Bayne, C. J., Carefoot, T. C. and Thompson, R. J. (1976). The physiological ecology of *Mytilus californianus* Conrad. 2. Adaptation to low oxygen tension and air exposure. *Oecologia* **22**, 229-250.

Bohning, D. E., Carter, B., Liu, S. S. and Pohost, G. M. (1990). PC-based system for retrospective cardiac and respiratory gating of NMR data. *Magn. Reson. Med.* **16**, 303-316.

Bokma, F. (2004). Evidence against universal metabolic allometry. *Funct. Ecol.* **18**, 184-187.

Braby, C. E. and Somero, G. N. (2006). Following the heart: temperature and salinity effects on heart rate in native and invasive species of blue mussels (genus *Mytilus*). *J. Exp. Biol.* **209**, 2554-2566.

Brody, S. (1945). *Bioenergetics and Growth*. New York: Reinhold Publishing Corp.

Brzęk, P., Bielawska, K., Książek, A. and Konarzewski, M. (2007). Anatomic and molecular correlates of divergent selection for basal metabolic rate in laboratory mice. *Physiol. Biochem. Zool.* **80**, 491-499.

Burpee, J. L., Bardsley, E. L., Dillaman, R. M., Watanabe, W. O. and Kinsey, S. T. (2010). Scaling with body mass of mitochondrial respiration from the white muscle of three phylogenetically, morphologically and behaviorally disparate teleost fishes. *J. Comp. Physiol. B* **180**, 967-977.

Carey, N., Sigwart, J. D. and Richards, J. G. (2013). Economies of scaling: more evidence that allometry of metabolism is linked to activity, metabolic rate and habitat. *J. Exp. Mar. Biol. Ecol.* **439**, 7-14.

Cella, M., Knibbe, C., Danhof, M. and Della Pasqua, O. (2010). What is the right dose for children? *Br. J. Clin. Pharmacol.* **70**, 597-603.

Couture, P. and Hulbert, A. J. (1995a). Membrane fatty acid composition of tissues is related to body mass of mammals. *J. Membr. Biol.* **148**, 27-39.

Couture, P. and Hulbert, A. J. (1995b). On the relationship between body mass, tissue metabolic rate and sodium pump activity in mammalian liver and kidney. *Am. J. Physiol.* **268**, R641-R650.

De Moreno, J. E. A., Moreno, V. J. and Brenner, R. R. (1976). Lipid metabolism of the yellow clam, *Mesodesma mactroides*: 2-polyunsaturated fatty acid metabolism. *Lipids* **11**, 561-566.

De Moreno, J. E. A., Moreno, V. J. and Brenner, R. R. (1977). Lipid metabolism of the yellow clam, *Mesodesma mactroides*: 3-saturated fatty acids and acetate metabolism. *Lipids* **12**, 804-808.

Else, P. L. and Hulbert, A. J. (1985). Mammals: an allometric study of metabolism at tissue and mitochondrial level. *Am. J. Physiol.* **248**, R415-R421.

Engelbrecht, F. M., Mari, F. and Anderson, J. T. (1974). Cholesterol. Determination in serum. A rapid direction method. *S.A. Med. J.* **48**, 250-256.

Farrell, A. P., Hammons, A. M., Graham, M. S. and Tibbits, G. F. (1988). Cardiac growth in rainbow trout, *Salmo gairdneri*. *Can. J. Zool.* **66**, 2368-2373.

Folch, J., Lees, M. and Stanley, G. H. S. (1957). A simple method for the isolation and purification of total lipids from animal tissues. *J. Biol. Chem.* **226**, 497-509.

Glazier, D. S. (2010). A unifying explanation for diverse metabolic scaling in animals and plants. *Biol. Rev.* **85**, 111-138.

Glazier, D. S. (2014). Metabolic scaling in complex living systems. *Systems* **2**, 451-540.

Glazier, D. S. (2015). Body-mass scaling of metabolic rate: what are the relative roles of cellular *versus* systemic effects? *Biology* **4**, 187-199.

Gonzalez, A., Pagé, B. and Weber, J.-M. (2015). Membranes as a possible pacemaker of metabolism in cypriniform fish: does phylogeny matter? *J. Exp. Biol.* **218**, 2563-2572.

Gudbjarnason, S., Doell, B., Oskardottir, G. and Hallgrimsson, J. (1978). Modification of cardiac phospholipids and catecholamine stress tolerance. In *Tocopherol, Oxygen and Biomembranes* (ed. C. de Duve and O. Hayaishi), pp. 297-310. Amsterdam: Elsevier.

Haggerty, C., Hoggard, N., Brown, D. S., Clapham, J. C. and Speakman, J. R. (2008). Intra-specific variation in resting metabolic rate in MF1 mice is not associated with membrane lipid desaturation in the liver. *Mech. Ageing Dev.* **129**, 129-137.

Hemmingsen, A. M. (1960). Energy metabolism as related to body size and respiratory surfaces, and its evolution. *Rep. Steno Mem. Hosp.* **9**, 1-110.

Hochachka, P. W., Darveau, C.-A., Andrews, R. D. and Suarez, R. K. (2003). Allometric cascade: a model for resolving body mass effects on metabolism. *Comp. Biochem. Physiol.* **134**, 675-691.

Hulbert, A. J. (2007). Membrane fatty acids as pacemakers of animal metabolism. *Lipids* **42**, 811-819.

Hulbert, A. J. (2010). Metabolism and longevity: is there a role for membrane fatty acids? *Integr. Comp. Biol.* **50**, 808-817.

Hulbert, A. J. and Else, P. L. (1999). Membranes as possible pacemakers of metabolism. *J. Theor. Biol.* **199**, 257-274.

Hulbert, A. J. and Else, P. L. (2000). Mechanisms underlying the cost of living in animals. *Annu. Rev. Physiol.* **62**, 207-235.

Hulbert, A. J. and Else, P. L. (2004). Basal metabolic rate: history, composition, regulation, and usefulness. *Physiol. Biochem. Zool.* **77**, 869-876.

Hulbert, A. J. and Else, P. L. (2005). Membranes and the setting of energy demand. *J. Exp. Biol.* **208**, 1593-1599.

Hulbert, A. J., Else, P. L., Manolis, S. C. and Brand, M. D. (2002). Proton leak in hepatocytes and liver mitochondria from archosaurs (crocodiles) and allometric relationships for ectotherms. *J. Comp. Physiol. B* **172**, 387-397.

Jimenez, A. G., Dasika, S. K., Locke, B. R. and Kinsey, S. T. (2011). An evaluation of muscle maintenance costs during fiber hypertrophy in the lobster *Homarus americanus*: are larger muscle fibers cheaper to maintain? *J. Exp. Biol.* **214**, 3688-3697.

Jimenez, A. G., Dillaman, R. M. and Kinsey, S. T. (2013). Large fiber size in skeletal muscle is metabolically advantageous. *Nat Commun.* **4**, 2150.

Johnston, I. A., Fernández, D. A., Calvo, J., Vieira, V. L. A., North, A. W., Abercromby, M. and Garland, T. (2003). Reduction in muscle fibre number during the adaptive radiation of notothenioid fishes: a phylogenetic perspective. *J. Exp. Biol.* **206**, 2595-2609.

Johnston, I. A., Abercromby, M., Vieira, V. L. A., Sigursteindóttir, R. J., Kristjánsson, B. K., Sibthorpe, D. and Skúlason, S. (2004). Rapid evolution of muscle fibre number in post-glacial populations of Arctic charr *Salvelinus alpinus*. *J. Exp. Biol.* **207**, 4343-4360.

Kerkhoff, A. J. (2012). Modeling metazoan growth and ontogeny. In *Metabolic Ecology A Scaling Approach* (ed. R. M. Sibly, J. H. Brown and A. Kodric-Brown), pp. 48-56. Wiley-Blackwell.

Kleiber, M. (1932). Body size and metabolism. *Hilgardia* **6**, 315-353.

Konarzewski, M. and Książek, A. (2013). Determinants of intra-specific variation in basal metabolic rate. *J. Comp. Physiol. B* **183**, 27-41.

Kooijman, S. A. L. M. (2010). *Dynamic Energy Budget Theory for Metabolic Organisation*. Cambridge: Cambridge University Press.

Kozłowski, J., Czarnołęski, M., François-Krassowska, A., Maciak, S. and Pis, T. (2010). Cell size is positively correlated between different tissues in passerine birds and amphibians, but not necessarily in mammals. *Biol. Lett.* **6**, 792-796.

Lannig, G., Cherkasov, A. S., Pörtner, H.-O., Bock, C. and Sokolova, I. M. (2008). Cadmium-dependent oxygen limitation affects temperature tolerance in eastern oysters (*Crassostrea virginica* Gmelin). *Am. J. Physiol. Regul. Integr. Comp. Physiol.* **294**, R1338-R1346.

Lannig, G., Eilers, S., Pörtner, H. O., Sokolova, I. M. and Bock, C. (2010). Impact of ocean acidification on energy metabolism of oyster, *Crassostrea gigas* – changes in metabolic pathways and thermal response. *Mar. Drugs* **8**, 2318-2339.

Maciak, S., Janko, K., Kotusz, J., Choleva, L., Boroń, A., Juchno, D., Kujawa, R., Kozłowski, J. and Konarzewski, M. (2011). Standard metabolic rate (SMR) is inversely related to erythrocyte and genome size in allopolyploid fish of the *Cobitis taenia* hybrid complex. *Funct. Ecol.* **25**, 1072-1078.

Maino, J. L. and Kearney, M. R. (2014). Ontogenetic and interspecific metabolic scaling in insects. *Am. Nat.* **184**, 695-701.

Mitchell, T. W., Ekroos, K., Blanksby, S. J., Hulbert, A. J. and Else, P. L. (2007). Differences in membrane acyl phospholipid composition between an endothermic mammal and an ectothermic reptile are not limited to any phospholipid class. *J. Exp. Biol.* **210**, 3440-3450.

Moses, M. E., Hou, C., Woodruff, W. H., West, G. B., Nekola, J. C. Zuo, W. and Brown, J. H. (2008). Revisiting a model of ontogenetic growth: estimating model parameters from theory and data. *Am. Nat.* **171**, 632-645.

Moyes, C. D., Mathieu-Costello, O. A., Tsuchiya, N., Filburn, C. and Hansford, R. G. (1997). Mitochondrial biogenesis during cellular differentiation. *Am. J. Physiol.* **272**, C1345-C1354.

Newton, T. J., Vaughn, C. C., Spooner, D. E., Nichols, S. J. and Arts, M. T. (2013). Profiles of biochemical tracers in unionid mussels across a broad geographical range. *J. Shellfish Res.* **32**, 497-507.

Philipp, E. E. R., Schmidt, M., Gsottbauer, C., Sanger, A. M. and Abele, D. (2008). Size- and age-dependent changes in adductor muscle swimming physiology of the scallop *Aequipecten opercularis*. *J. Exp. Biol.* **211**, 2492-2501.

Porter, R. K. (2001). Allometry of mammalian cellular oxygen consumption. *Cell. Mol. Life Sci.* **58**, 815-822.

Porter, R. K. and Brand, M. D. (1995). Cellular oxygen consumption depends on body mass. *Am. J. Physiol.* **269**, R226-R228.

Porter, R. K., Hulbert, A. J. and Brand, M. D. (1996). Allometry of mitochondria proton leak: influence of membrane surface area and fatty acid composition. *Am. J. Physiol.* **271**, R1550-R1560.

Prothero, J. (1979). Heart weight as a function of body weight in mammals. *Growth* **43**, 139-150.

Rouillon, G. and Navarro, E. (2003). Differential utilization of species of phytoplankton by the mussel *Mytilus edulis*. *Acta Oecol.* **24**, S299-S305.

Rubner, M. (1883). Ueber den einfluss der körpergrösse auf stoff- und kraftwechsel. *Z. Biol.* **19**, 535-562.
Sargent, J. R. and Falk-Petersen, S. (1988). The lipid biochemistry of calanoid copepods. In *Biology of Copepods. Proceedings of the Third International Conference on Copepoda* (ed. G. Boxshall and H. K. Schminke), pp. 101-114. Springer.
Savage, V. M., Allen, A. P., Brown, J. H., Gillooly, J. F., Herman, A. B., Woodruff, W. H. and West, G. B. (2007). Scaling of number, size, and metabolic rate of cells with body size in mammals. *Proc. Natl. Acad. Sci. USA* **104**, 4718-4723.
Savina, M. V. Gamper, N. L. and Brailovskaya, I. V. (1997). Dependence of the hepatocyte respiratory rate on the body mass in poikilothermal vertebrates. *J. Evol. Biochem. Physiol.* **33**, 339-343 (in Russian).
Schmidt-Nielsen, K. (1984). *Scaling. Why is Animal Size so Important?* Cambridge, UK: Cambridge University Press.
Seo, E., Ohishi, K., Maruyama, T., Imaizumi-Ohashi, Y., Murakami, M. and Seo, Y. (2014a). Testing the constant-volume hypothesis by magnetic resonance imaging of *Mytilus galloprovincialis* heart. *J. Exp. Biol.* **217**, 964-973.
Seo, E., Ohishi, K., Maruyama, T., Imaizumi-Ohashi, Y., Murakami, M. and Seo, Y. (2014b). Magnetic resonance imaging analysis of water flow in the mantle cavity of live *Mytilus galloprovincialis*. *J. Exp. Biol.* **217**, 2277-2287.
Sidell, B. D., Driedzic, W. R., Stowe, D. B. and Johnston, I. A. (1987). Biochemical correlations of power development and metabolic fuel preferenda in fish hearts. *Physiol. Zool.* **60**, 221-232.
Sidorov, V. S., Lizenko, E. I., Bolgova, O. M. and Nefedova, Z. A. (1972). *Fish Lipids. 1. Analysis Technique*. Petrozavodsk: Karelian Branch of the USSR Academy of Science (in Russian).
Strahl, J. and Abele, D. (2010). Cell turnover in tissues of the long-lived ocean quahog *Arctica islandica* and the short-lived scallop *Aequipecten opercularis*. *Mar. Biol.* **157**, 1283-1292.
Strickland, J. D. and Parsons, T. R. (1968). A practical handbook of seawater analysis. *Bull. Fish. Res. Board Can.* **167**, 1-311.
Szabó, A., Fébel, H., Horn, P., Bázár, G. Y. and Romvári, R. (2006). Ontogenic development of the fatty acyl chain composition of the turkey (*Meleagris gallopavo*) *pectoralis superficialis* muscle membranes (an allometric approach). *Acta Biol. Hung.* **57**, 165-180.
Trumble, S. J. and Kanatous, S. B. (2012). Fatty acid use in diving mammals: more than merely fuel. *Front. Physiol.* **3**, 184.
Tsyganov, E. P. (1971). Method of direct lipids methylation after TLC without elution with silica gel. *Lab. Delo* **6**, 490-493 (in Russian).
Viso, A.-C. and Marty, J.-C. (1993). Fatty acids from 28 marine microalgae. *Phytochem.* **34**, 1521-1533.
Volkman, J. K., Johns, R. B., Gillan, F. T., Perry, G. J. and Bavor, H. J. (1980). Microbial lipids of an intertidal sediment—I. Fatty acids and hydrocarbons. *Geochim. Cosmochim. Acta* **44**, 1133-1143.
West, G. B. and Brown, J. H. (2005). The origin of allometric scaling laws in biology from genomes to ecosystems: towards a quantitative unifying theory of biological structure and organization. *J. Exp. Biol.* **208**, 1575-1592.
West, G. B., Brown, J. H. and Enquist, B. J. (1997). A general model for the origin of allometric scaling laws in biology. *Science* **276**, 122-126.
West, G. B., Woodruff, W. H. and Brown, J. H. (2002). Allometric scaling of metabolic rate from molecules and mitochondria to cells and mammals. *Proc. Natl. Acad. Sci. USA* **99**, 2473-2478.
White, C. R. and Kearney, M. R. (2013). Determinants of inter-specific variation in basal metabolic rate. *J. Comp. Physiol. B* **183**, 1-26.
Winberg, G. G. (1956). *Rate of Metabolism and Food Requirements of Fish*. Minsk: Nauchnye Trudy Belorusskovo Gosudarstvennovo Universiteta imeni V.I. Lenina (in Russian).
Windisch, H. S., Kathöver, R., Pörtner, H.-O., Frickenhaus, S. and Lucassen, M. (2011). Thermal acclimation in Antarctic fish: transcriptomic profiling of metabolic pathways. *Am. J. Physiol. Regul. Integr. Comp. Physiol.* **301**, R1453-R1466.
Zeuthen, E. (1947). Body size and metabolic rate in the animal kingdom with special regard to the marine micro-fauna. *C. R. Trav. Lab. Carlsberg Ser. Chim.* **26**, 17-161.
Zhang, Y., Huang, Q., Liu, S., He, D., Wei, G. and Luo, Y. (2014). Intraspecific mass scaling of metabolic rates in grass carp (*Ctenopharyngodon idellus*). *J. Comp. Physiol. B* **184**, 347-354.
Zittier, Z. M. C., Bock, C., Lannig, G. and Pörtner, H.-O. (2015). Impact of ocean acidification on thermal tolerance and acid–base regulation of *Mytilus edulis* (L.) from the North Sea. *J. Exp. Mar. Biol. Ecol.* **473**, 16-25.